UCRL-CONF-231949

ELECTROMAGNETIC SIMULATIONS OF LINEAR PROTON ACCELERATOR STRUCTURES USING DIELECTRIC WALL ACCELERATORS

S.D. Nelson, B.R. Poole, G.J. Caporaso

June 20, 2007

2007 Particle Accelerator Conference
Albuquerque, NM, United States
June 25, 2007 through June 29, 2007

ELECTROMAGNETIC SIMULATIONS OF LINEAR PROTON ACCELERATOR STRUCTURES USING DIELECTRIC WALL ACCELERATORS

S.D. Nelson, B.R. Poole, and G.J. Caporaso
Lawrence Livermore National Laboratory, Livermore CA 94551

Abstract

Proton accelerator structures for medical applications using Dielectric Wall Accelerator (DWA) technology allow for the utilization of high electric field gradients on the order of 100 MV/m to accelerate the proton bunch. Medical applications involving cancer therapy treatment usually desire short bunch lengths on the order of hundreds of picoseconds in order to limit the extent of the energy deposited in the tumor site (in 3D space, time, and deposited proton charge). Electromagnetic simulations of the DWA structure, in combination with injections of proton bunches have been performed using 3D finite difference codes in combination with particle pushing codes. Electromagnetic simulations of DWA structures includes these effects and also include the details of the switch configuration and how that switch time affects the electric field pulse which accelerates the particle beam.

INTRODUCTION

DWA-based structures have the advantage over conventional linear accelerator structures of having a high gradient present at the accelerator's beampipe wall since the geometry of the DWA reduces the spatial overhead. This allows the wall electric field to be the predominant factor in determining the on-axis accelerating field. However, such designs have typically experienced a parasitic effect [1] which reduced the acceleration field due to the closure of the magnetic field lines in undesirable planes. The profiled dielectric radial transmission line based Blumlein structure presented here exhibits a constant impedance and magnetic field lines that close in the plane thus preventing the parasitic effect and allowing for a square-wave operation consistent with standard transmission line theory.

PROFILED DIELECTRIC GEOMETRY

Consider profiled radial line has a permittivity profile [2], $\varepsilon_r(r)$, which follows:

$$\varepsilon_r(r) = \varepsilon_{\max}\left(\frac{a}{r}\right)^2$$

Then by applying this to the standard radial transmission line equation [3] yields an impedance, *Z(r)*, which is:

$$Z(r) = \sqrt{\frac{\mu_0\mu_r}{\varepsilon_0\varepsilon_r(r)}}\,\frac{d}{2\pi r} \approx \frac{60}{\sqrt{\varepsilon_r}}\,\frac{d}{r} = \frac{60}{\sqrt{\varepsilon_{\max}}}\,\frac{d}{a}$$

and is constant with respect to radius. Note that ε_{max} limits the maximum dielectric permittivity in the configuration, *a* is the inner radius of the configuration, and *d* is the transmission line thickness. Since the direction of propagation is radial, and the electric field points from the lower transmission line plate to the upper transmission line plate, then the magnetic field is azimuthal. Setting nominal values for the above parameters yields Figure 1.

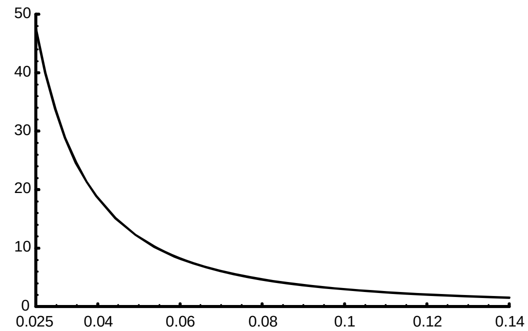

Figure 1: Using nominal values for the permittivity in the profiled radial line versus radius (in meters) given ε_{max} = 47.6, *a* = 25mm, and *d* = 1mm, yields Z(r)=0.347Ω.

From this dielectric constant, the radial velocity and position at time *t* follows from:

$$v(r) = \frac{c}{\sqrt{\varepsilon_r}} = \frac{c}{\sqrt{\varepsilon_{\max}}}\,\frac{r}{a} = \frac{dr}{dt}$$

$$r(t) = a e^{ct/a\sqrt{\varepsilon_{\max}}}$$

then inverting, yields:

$$t(r) = \frac{a\sqrt{\varepsilon_{\max}}}{c}\ln\left(\frac{r}{a}\right)$$

However, for conventional fabrication techniques it is envisioned that a discrete graded dielectric profile would be used to construct the profiled dielectric utilized in the radial line as shown in Figure 2.

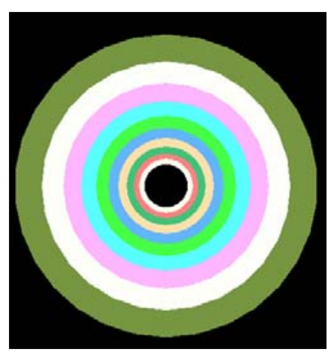

Figure 2: Typical radial grading process for discrete dielectric layers as used in the profiled radial line.

As a result of the grading process, the extents of the permittivity profile have to be adjusted such that the extents across the material allow for the same propagation times. By adjusting the dielectric constants such that the integral over the span of each dielectric subsection is equalized, the resulting permittivity profile is obtained and is shown in Figure 3.

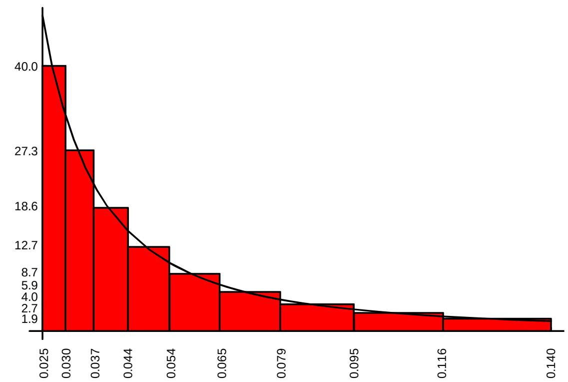

Figure 3: Adjusted relative permittivity profile versus radius (in meters) after the descretization process.

The motivation in setting the permittivities in the radial profile is to maintain a constant impedance w.r.t. radius. The radial span of each subsection in the dielectric is selected such that the propagation time through each subsection is the same. This effect is shown in Figure 4.

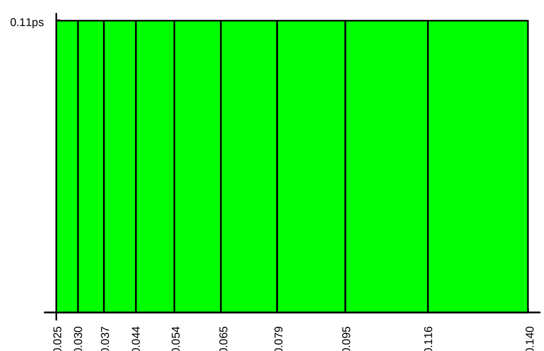

Figure 4: Time spent in each dielectric subsection showing the propagation time of the wavefront through the subsection vs. radius (in meters).

The radial transmission line stack is then arranged in a Blumlein configuration and is placed in a sealed box, with flanges and foils on each end for the beampipe.

ELECTROMAGNETIC SIMULATIONS

Electromagnetic (EM) simulations using FDTD (finite difference time domain) [4] modeling produce the spatial snapshot at a point in time along the beam axis as shown in Figure 5. The switches are arranged azimuthally with a switch on-resistance of 0.25Ω. For these simulations, the beam current is small (100mA) and so the beam loading affects are presumed to be small and are ignored.

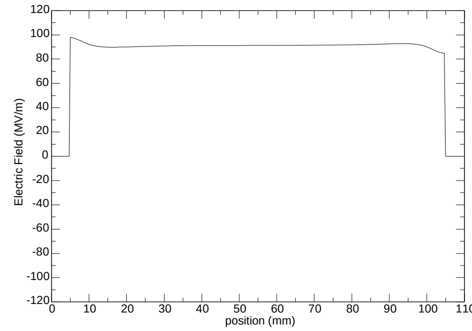

Figure 5: The on-axis electric field at a snapshot in time shows the uniformity of the field across the structure. Note that the two discontinuities are foils at the entrance and exit to the accelerator.

When applying an acceleration schedule to track an accelerating proton bunch (discussed in more detail in the next section), the on-axis time domain waveform in the middle of the structure obtained from the EM simulation is shown in Figure 6.

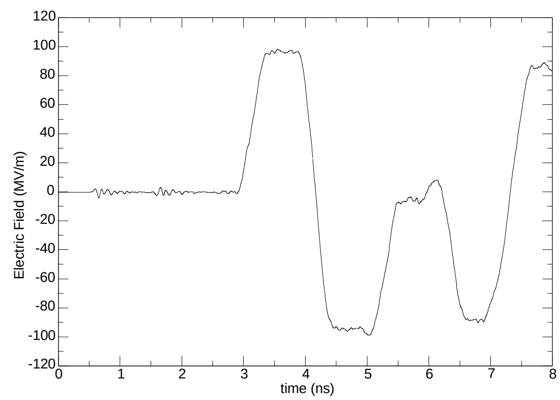

Figure 6: The on-axis time domain waveform in the middle of the structure shows the acceleration pulse for the proton bunch.

PARTICLE SIMULATIONS

The timing of the proton bunch entering the accelerator cell should be set to capture the beam over the acceptance of the cell and accelerate it through the cell. To illustrate the effects of proton bunch propagation in the simplest configuration (with all switches firing simultaneously), an arbitrarily high proton input beam energy of 50MeV is selected such that the proton bunch crosses the 10cm radial stack during the positive (accelerating) portion of the 1ns temporal waveform ($\beta\approx0.3$). From simulations [1], the resulting output beam from the 10cm radial stack has gained ~ 9MeV of energy and has only increased in size by ½% and r′ < 2 milliradians.

For a lower energy proton bunch entering the cell (0.78MeV), an acceleration schedule is required for this short pulse configuration since the transit time across the accelerator cell for a low energy proton bunch exceeds the temporal pulse width of the acceleration pulse. For this acceleration process, the acceleration schedule methodology described in [1] is used and is shown in Figure 7.

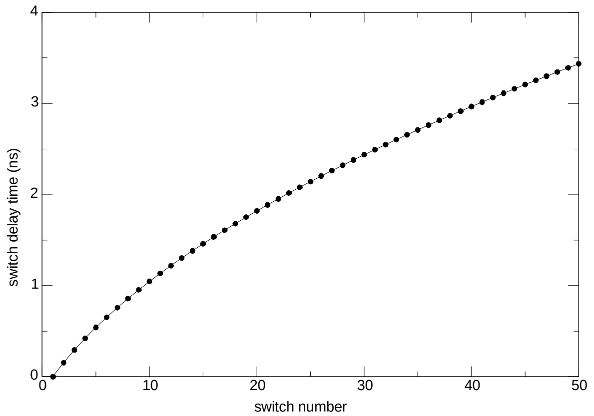

Figure 7: For low energy proton beams entering the accelerator cell, this acceleration schedule is used to control the switch closure rate longitudinally down the cell.

The resulting phase space at the output for the 0.78MeV input proton bunch is shown in Figure 8. The proton beam entering the accelerator cell is 1cm in diameter and the beampipe diameter is 4cm.

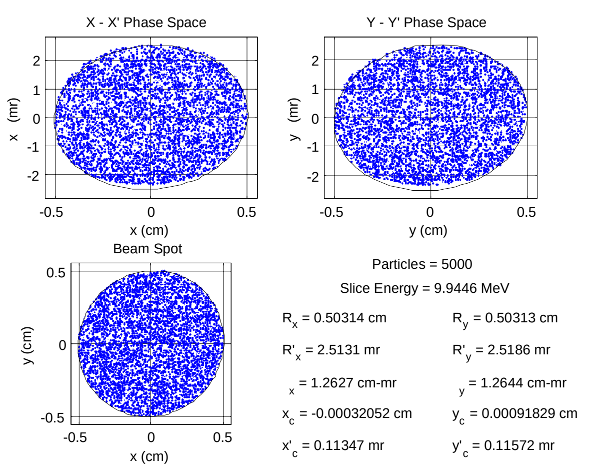

Figure 8: The result of accelerating a 0.78MeV 1cm dia. proton bunch through the structure using an acceleration schedule produces a well behaved phase space and beam spot size at the output of the 10cm radial stack. The beam gains ~ 9.2MeV of energy.

The particles are accelerated over the span of the DWA that is active according to the switch closure rate driving the accelerating electric field on the wall of the accelerator. Thus, this acceleration region has to stay in lock-step with the future locations of the particles due to their acceleration and includes the transit times of the EM pulses according to the delay times shown in Figure 4.

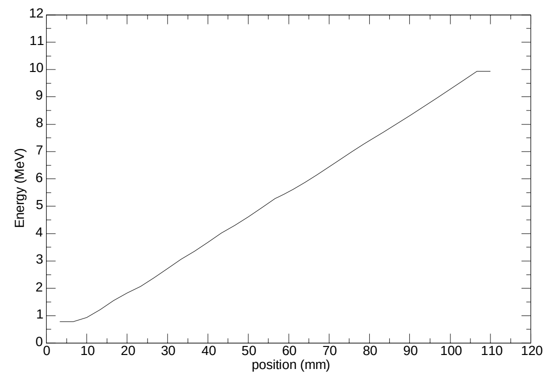

Figure 9: The energy gain of the proton bunch along the acceleration axis shows the energy increase during acceleration. The changes in slope in the figure (at 7mm and 107mm) are foils placed at the entrance and exit of the accelerator.

CONCLUSION

Using radial transmission line structures in a Blumlein configuration, in combination with a profiled dielectric for constant impedance, allows for rise-time preserving pulses with high resolution flat tops to accelerate a charged particle beam. In this paper, protons where accelerated but the same technique applies to any charged particle as long as the acceleration schedule (relative switch timing) is adjusted according to the rate at which the particles increase velocity (a.k.a. acceleration). Radial configurations have the advantage of constraining the magnetic field inside of the transmission line layer in the classic radial configuration. Simultaneous switching allows for the input of high energy particle beams, where as applying an acceleration schedule in the radial stack allows for the input of low energy beams.

ACKNOWLEDGEMENTS

This work was performed under the auspices of the U.S. Department of Energy by University of California, Lawrence Livermore National Laboratory under Contract W-7405-Eng-48.

REFERENCES

[1] B.R. Poole, et. al., “Particle Simulations of a Linear Dielectric Wall Proton Accelerator,” Particle Accelerator Conference 2007 (PAC07), Albuquerque, NM, June 25-29, 2007, TUPAS060.

[2] G.J. Caporaso, et. al., “High Gradient Induction Accelerator,” Particle Accelerator Conference 2007 (PAC07), Albuquerque, NM, June 25-29, 2007, TUYC02.

[3] N. Marcuvitz, “Waveguide Handbook,” Peregrinus Ltd., 1993, ISBN 0-86341-058-8, pp. 32,91.

[4] xFDTD from RemCom Inc., State College, Pennsylvania.